Supporting information

Multilayer Structured AgNW/WPU-MXene Fiber Strain Sensors with Ultrahigh Sensitivity and Wide Operating Range for Wearable Monitoring and Healthcare

Jun-Hong Pu, Xing Zhao, Xiang-Jun Zha, Lu Bai, Kai Ke, Rui-Ying Bao, Zheng-Ying Liu, Ming-Bo Yang, Wei Yang*

College of Polymer Science and Engineering, Sichuan University, State Key Laboratory of Polymer Materials Engineering, Chengdu, 610065, Sichuan, People's Republic of China.

*Corresponding author. Tel.: + 86 28 8546 0130; fax: + 86 28 8546 0130.

E-mail addresses: weiyang@scu.edu.cn (W Yang)

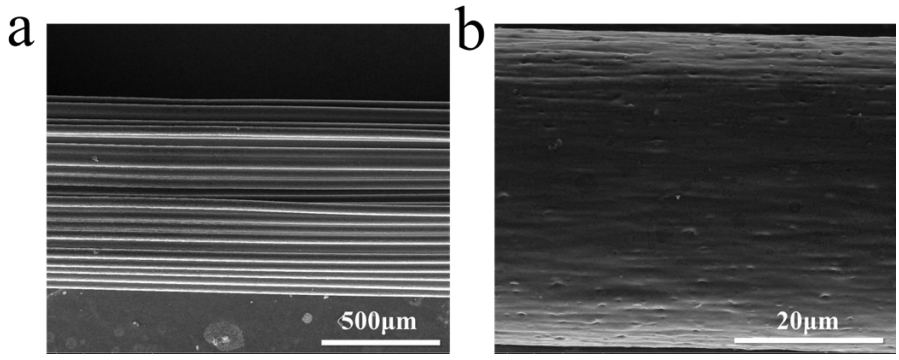

Figure S1. (a) SEM image of the surface of HPUF with coalesced filament structure. (b) High-magnification SEM image of the surface of one filament.

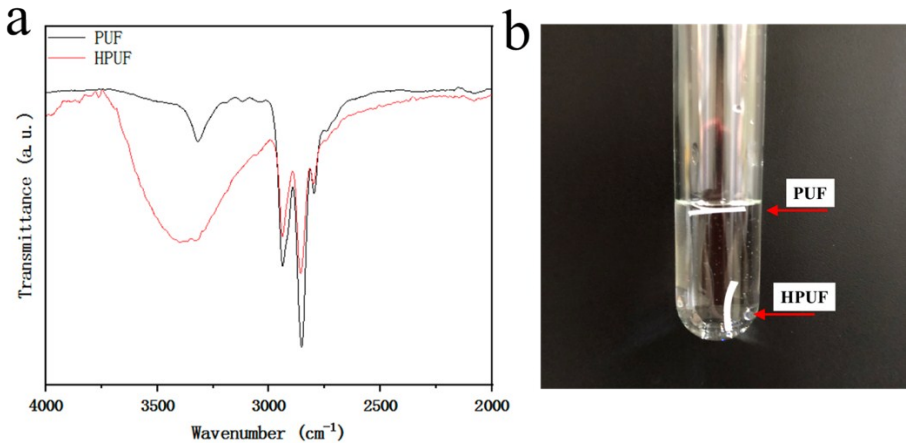

Figure S2. (a) FTIR spectra of PUF and HPUF. (b) Optical image showing different water infiltration ability of PUF and HPUF

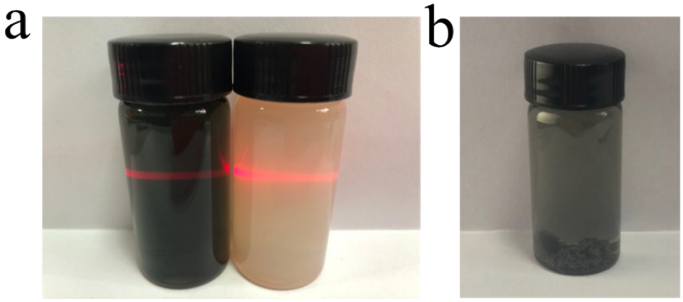

Figure S3. (a) Tyndall effect of MXene and AgNW/WPU inks. (b) Flocculation of AgNWs and MXenes.

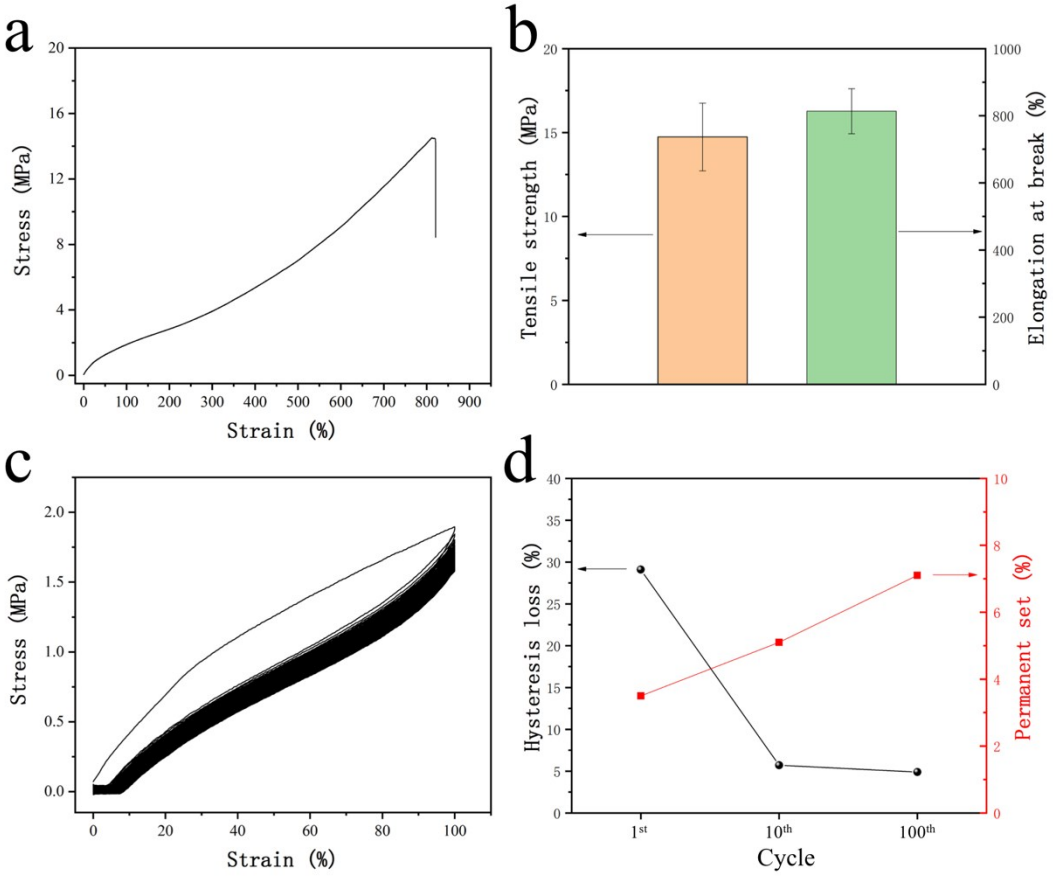

Figure S4. (a) The stress-strain curve of the fiber strain sensor. (b) The tensile strength and elongation at break of the fiber sensor. (c) The stress-strain curves of cycle strain loading and unloading test. (d) The hysteresis loss and permanent set of the fiber sensor in the 1st, 10th, and 100th cycles.

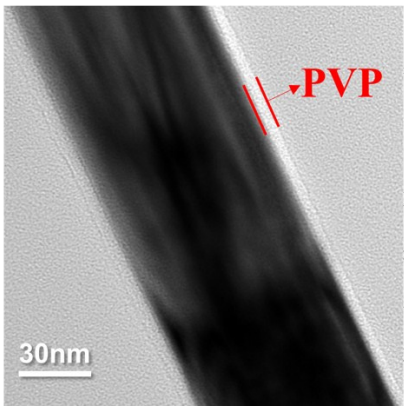

Figure S5. The TEM image of AgNW showing a very thin layer of PVP on the surface

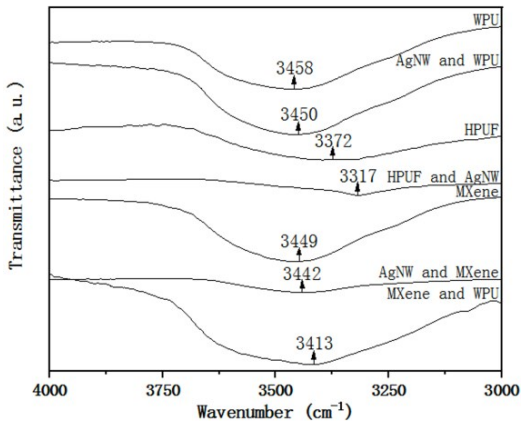

Figure S6. FTIR spectra of WPU, HPUF, MXene, AgNW and WPU, HPUF and AgNW, AgNW and MXene, and MXene and WPU.

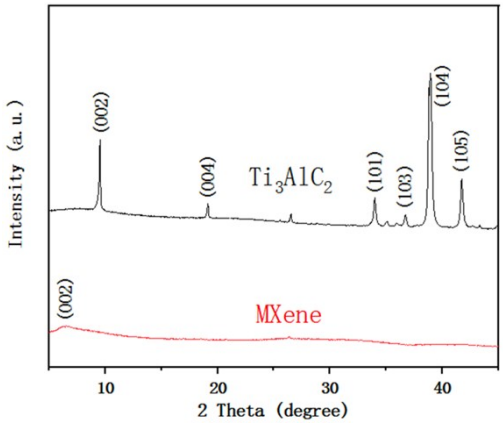

Figure S7. XRD patterns of Ti_3AlC_2 and MXene.

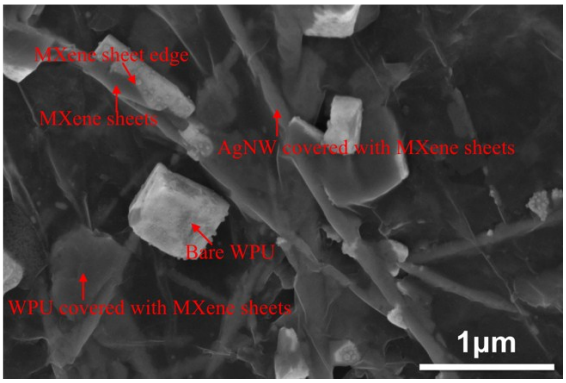

Figure S8. High-magnification SEM image showing MXene layer tightly covered on AgNW/WPU layer.

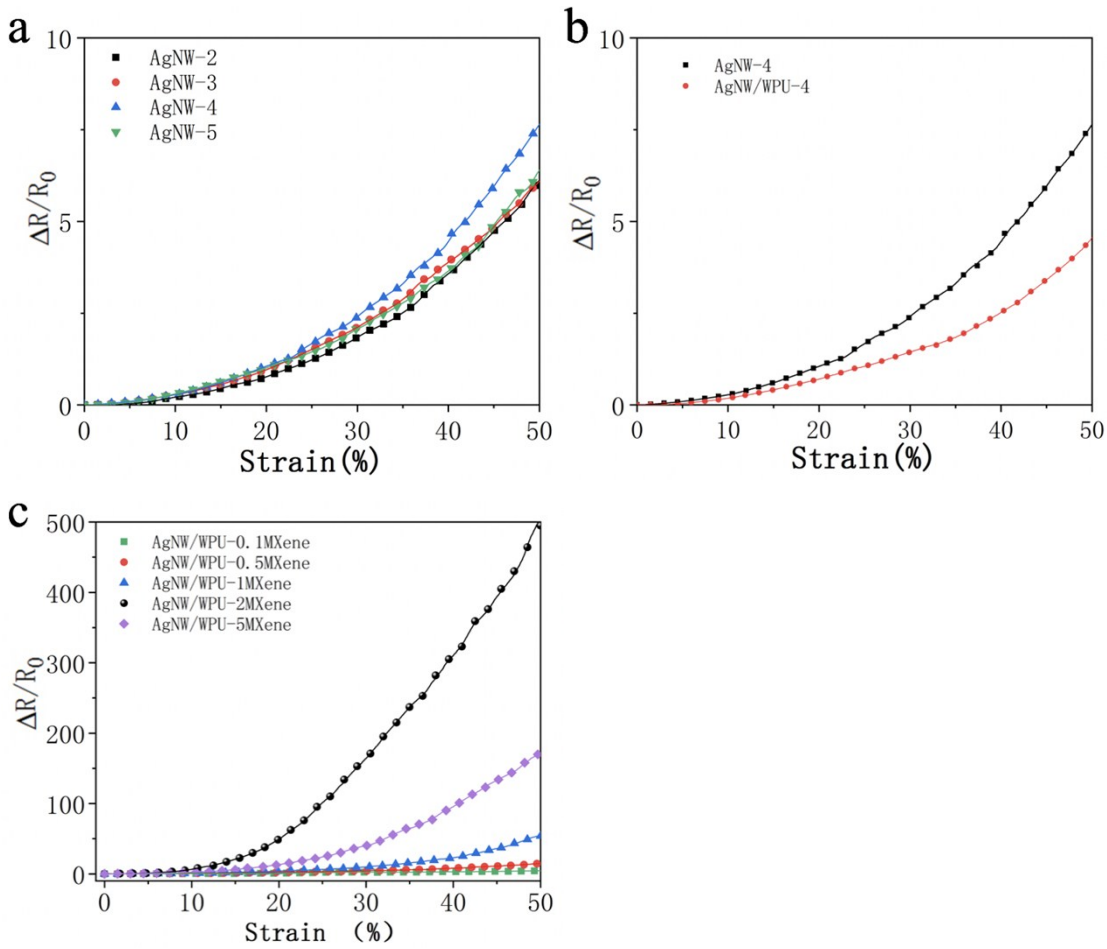

Figure S9. (a) Typical relative resistance−strain curves of HPUFs dip-coating with AgNW/WPU ink for different times (2 to 5 times). (b) Typical relative resistance−strain curves of HPUFs dip-coating with AgNW ink and AgNW/WPU ink for 4 times. (c) Typical relative resistance−strain curves of HPUFs dip-coating with AgNW/WPU ink and MXene inks with different concentrations (0.1, 0.5, 1, 2, and 5 mg/mL) for 4 times.

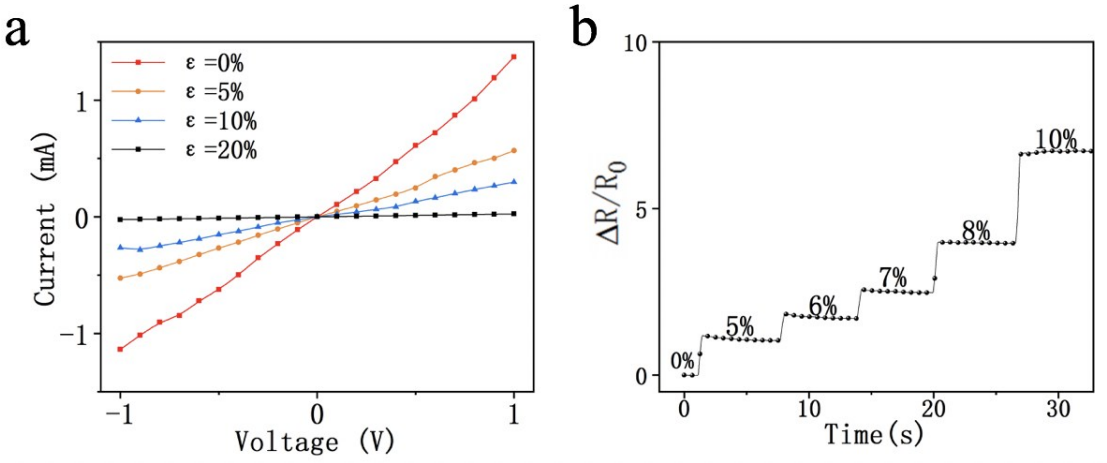

Figure S10. (a) Current−voltage curves of the fiber strain sensor at different strains (0%, 5%, 10% and 20%). (c) Relative resistance changes at various applied strains ranging from 0% to 10%.

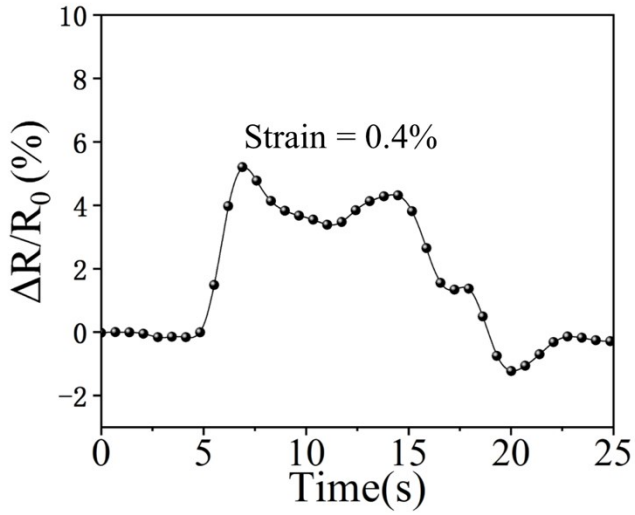

Figure S11. The lower limit detection of this fiber strain sensor.

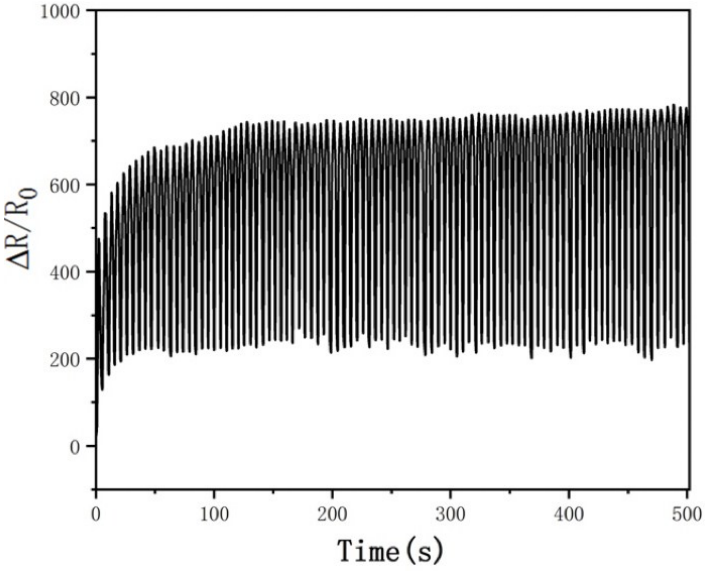

Figure S12. Durability test under repeated strains of 50% for around 100 cycles.

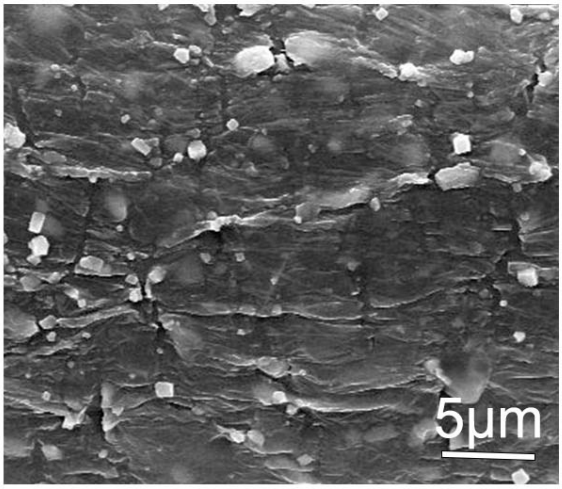

Figure S13. Surface SEM image of the fiber strain sensor recover after large deformation.

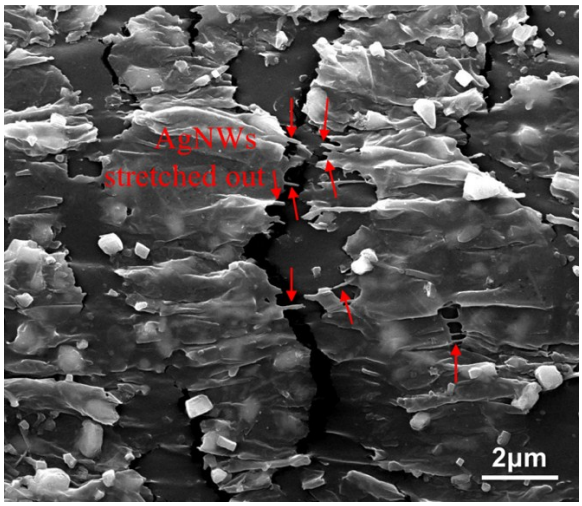

Figure S14. High-magnification SEM image showing AgNWs were stretched at the new generated crack edge.

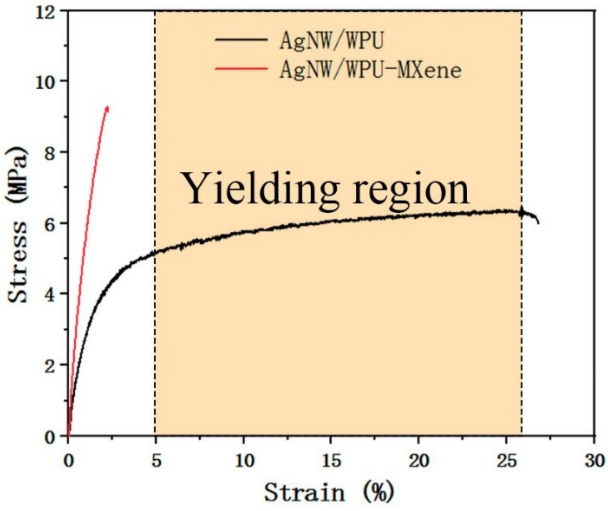

Figure S15. Typical stress−strain curves of AgNW/WPU film and AgNW/WPU-MXene film fabricated by layer-by-layer cast-coating for 4 times.

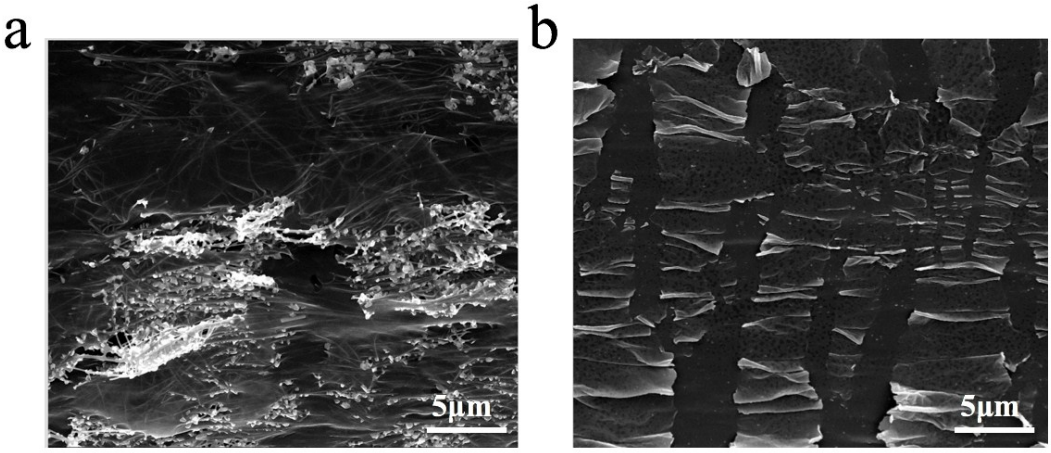

Figure S16. SEM images of the surface of HPUFs with (a) AgNW/WPU layers and (b) MXene layers at 50% strain states.

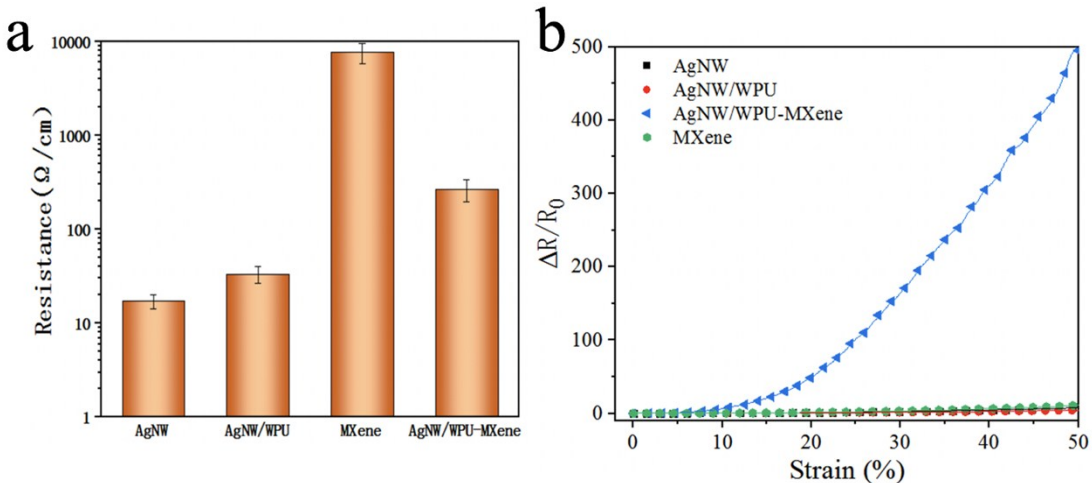

Figure S17. (a) Initial resistances of HPUFs coated with different layers. (b) Typical relative resistance−strain curves of HPUFs dip-coating with AgNW ink, AgNW/WPU ink, AgNW/WPU ink and MXene inks, and MXene ink for 4 times.